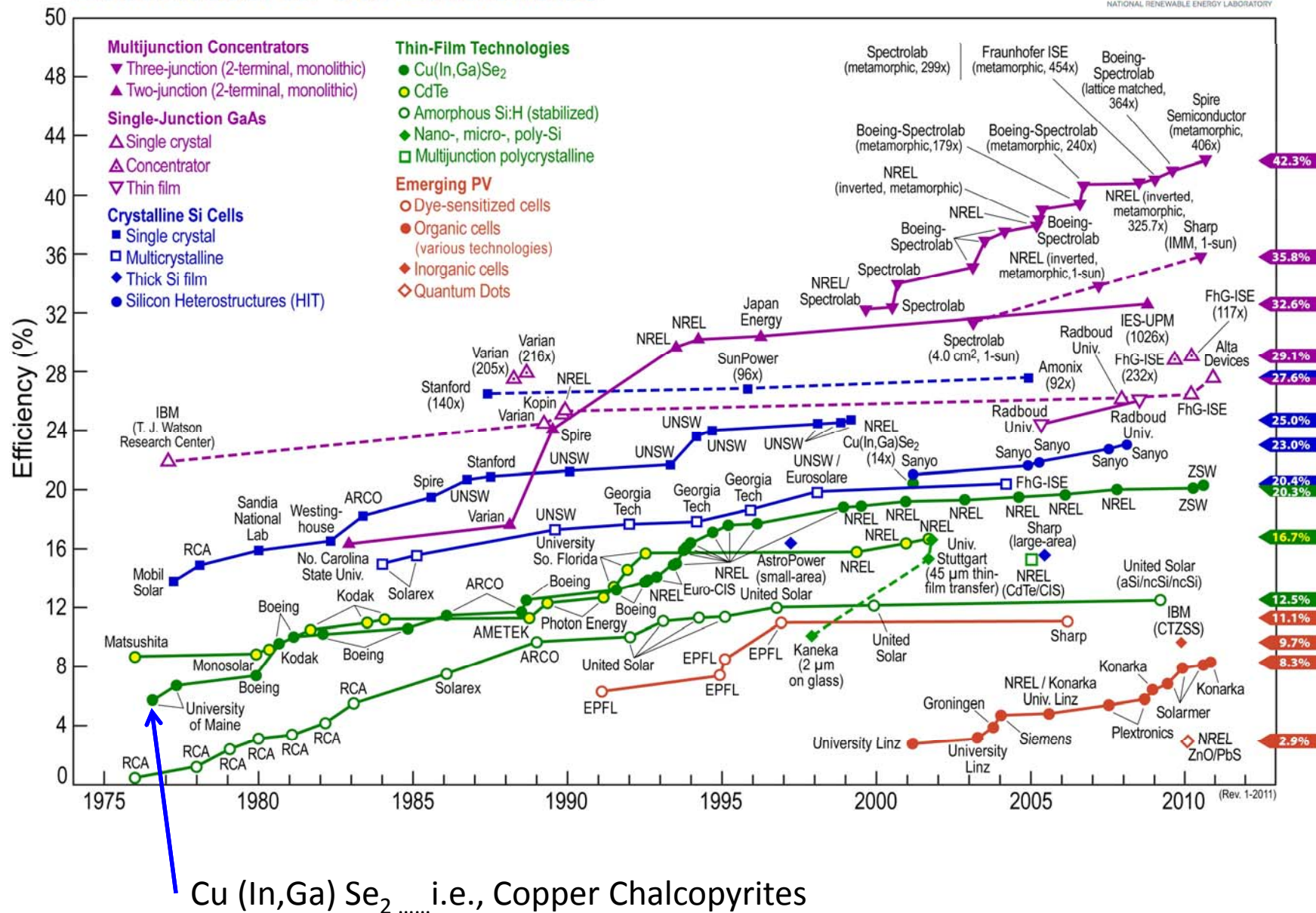


# CIGS Photovoltaic Technology

- materials
- devices
- methods

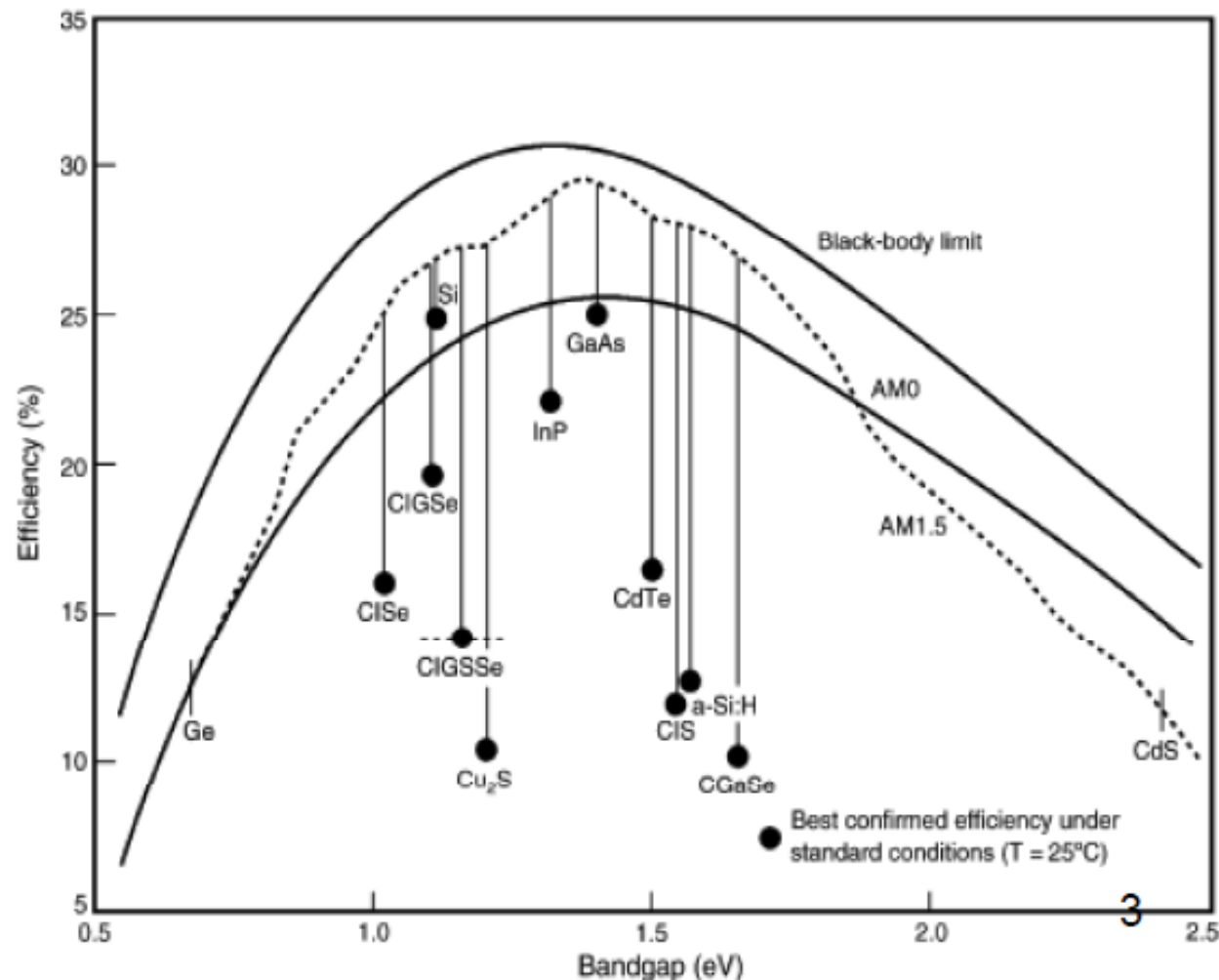
## Best Research-Cell Efficiencies



Cu (In,Ga) Se<sub>2</sub> .... i.e., Copper Chalcopyrites

## Solar photovoltaics R&D at the tipping point: A 2005 technology overview

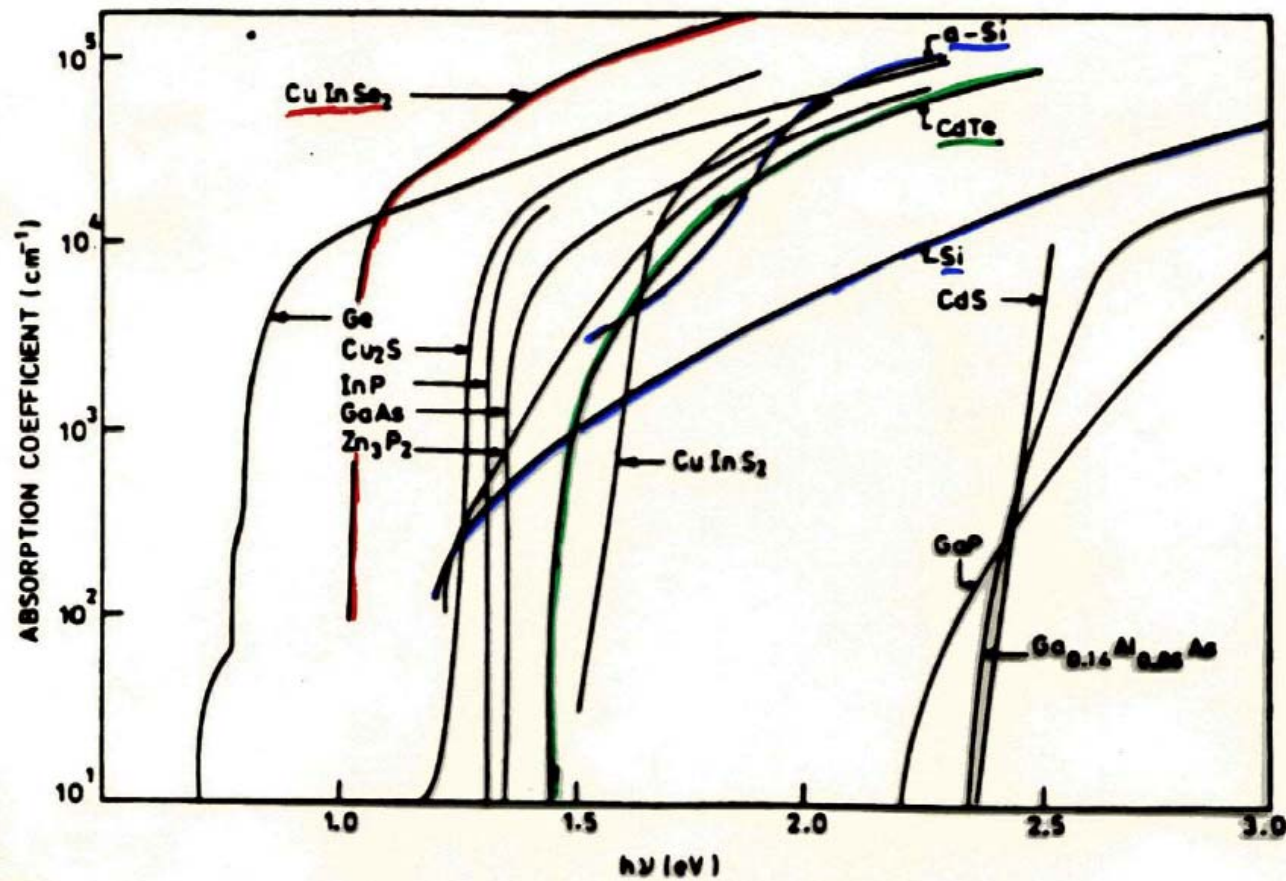
Lawrence L. Kazmerski



	Laboratory Cell Efficiency	Best in Class Production Module	Typical Production
CPV	~40%	~32%	~29%
c-Si	~25%	~20%	~18%
mc-Si	~20%	~17%	~14%
CIGS	~20%	~11%	~11%
CdTe	~16%	~11%	~11%
a-Si	~12%	~8%	~8%
OPV	~7%	~4%	~2%

Presentation by John Lushetsky, DOE Solar Program, Grid Parity and Beyond –Challenges and Opportunities, *NIST Workshop for Advances in PV Technologies and Measurements*, May 12, 2010, Denver, CO

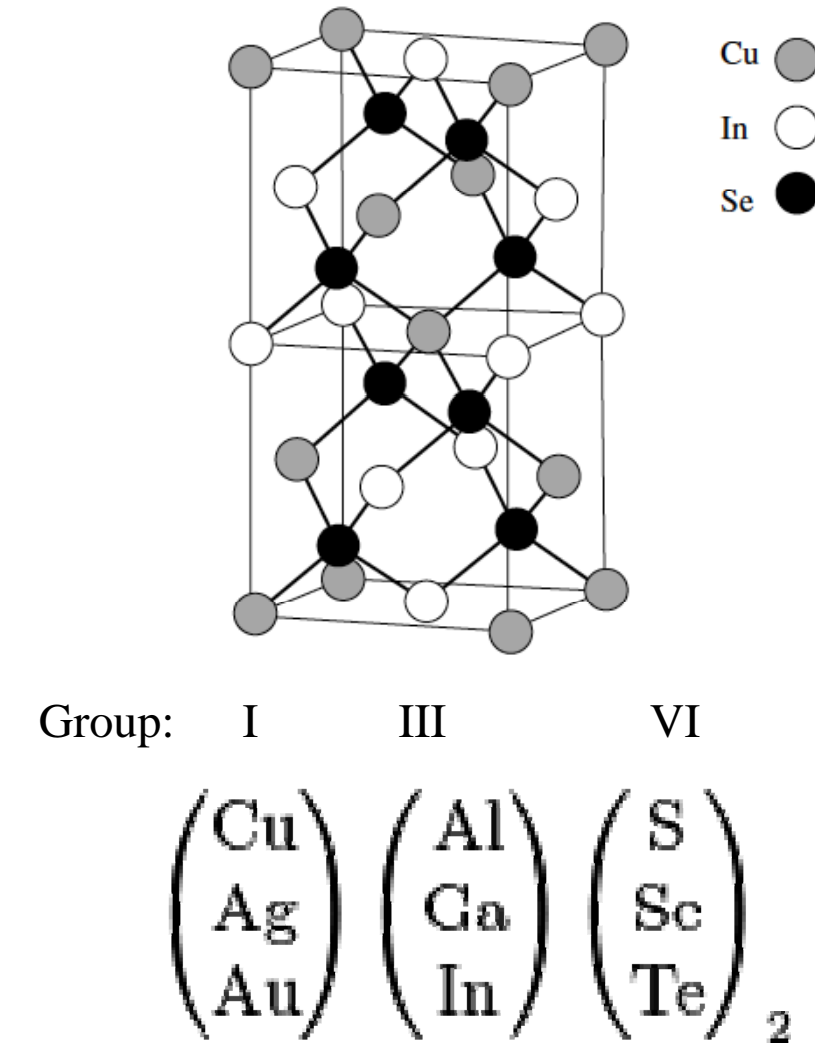
## Absorption spectra of various semiconductors



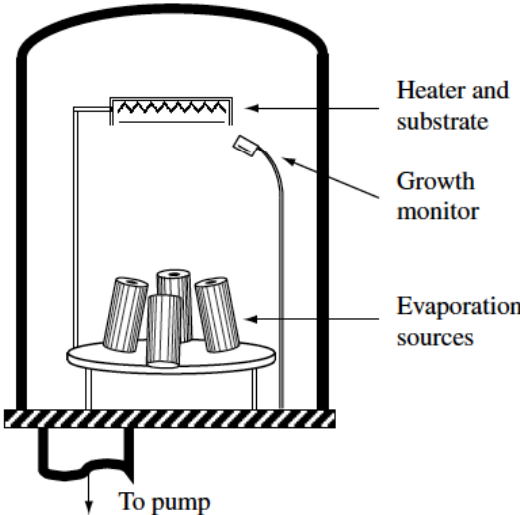
Courtesy of Al Compaan

# Crystal Structure

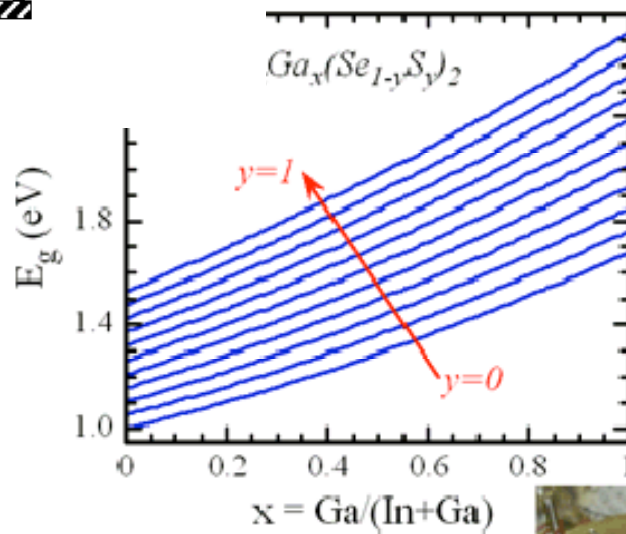
- $\text{CuInSe}_2$  and  $\text{CuGaSe}_2$  have the chalcopyrite lattice structure.
- Diamond-like structure similar to the sphalerite (zincblende) structure but with an ordered substitution of the group I (Cu) and group III (In or Ga) elements on the group II (Zn) sites of sphalerite.
- Tetragonal unit cell,  $c/a$  close to 2.
- Deviation from  $c/a = 2$  due to different strengths for Cu–Se and In–Se, Ga–Se bonds.

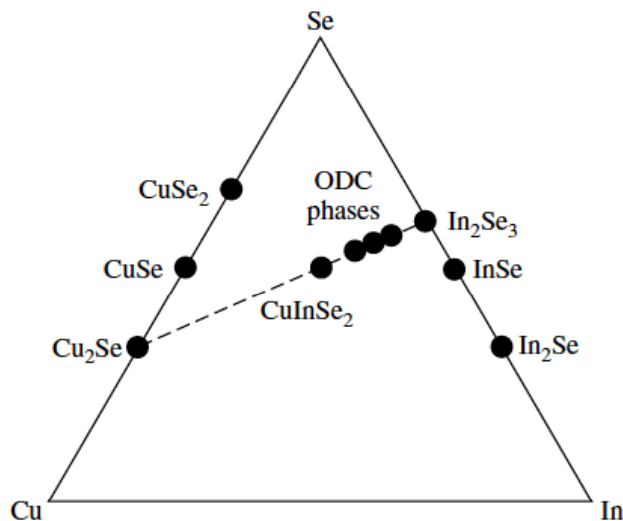


From “ $\text{Cu}(\text{InGa})\text{Se}_2$  Solar Cells”, by Shafarman and Stolt, and Wikipedia

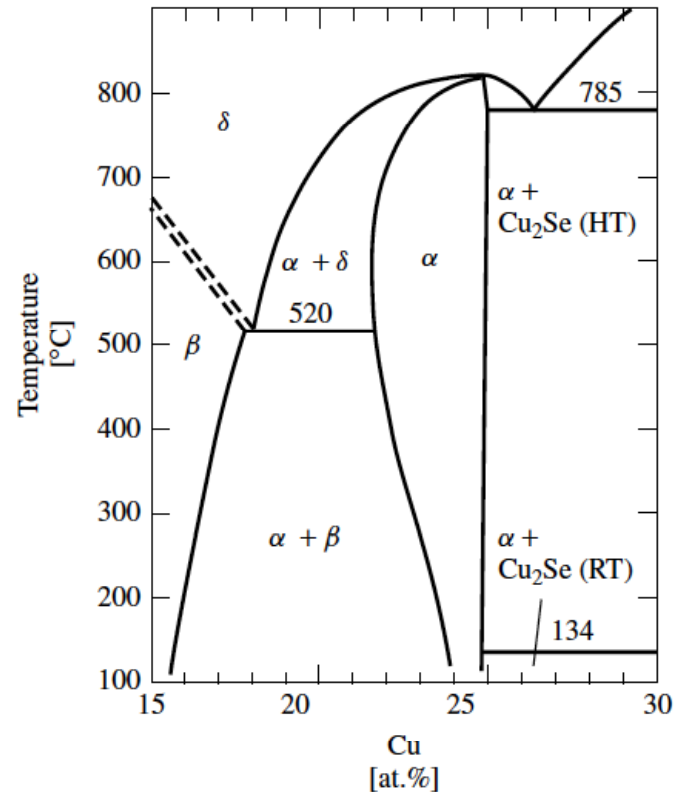


*At IEC Cu(InGa)(SeS)<sub>2</sub> films are deposited by five source elemental evaporation (right) and by the reaction of Cu-Ga-In films in H<sub>2</sub>Se and H<sub>2</sub>S*





Ternary phase diagram of the Cu–In–Se system. Thin-film composition is near the pseudobinary Cu<sub>2</sub>Se–In<sub>2</sub>Se<sub>3</sub> tie-line



Pseudobinary In<sub>2</sub>Se<sub>3</sub>–Cu<sub>2</sub>Se equilibrium phase diagram for compositions around the CuInSe<sub>2</sub> chalcopyrite phase, denoted  $\alpha$ . The  $\delta$  phase is the high-temperature sphalerite phase, and the  $\beta$  phase is an ordered defect phase (ODC). Cu<sub>2</sub>Se exists as a room-temperature (RT) or high-temperature (HT) phase. (After G\"odecke T, Haalboom T, Ernst F, Z. Metallkd. **91**, 622–634 (2000) [32])

# History of CIGS

- $\text{CuInSe}_2$  was first synthesized and characterized in 1953 by Hahn et al.
- Solar cell-relevant work started at Bell Laboratories in the early 1970s. A wide selection of ternary chalcopyrite crystals were grown and characterized (structural, electronic, and optical properties).
- The first  $\text{CuInSe}_2$  solar cells were made by evaporating *n-type CdS onto p-type single*
- crystals of  $\text{CuInSe}_2$  by Shay et al. in 1974. Potential as near-infrared photodetectors since their spectral response was broader and more uniform than Si photodetectors.
- Shay et al. in 1975, increased the solar cell efficiency to 12% as measured under outdoor illumination “on a clear day in New Jersey”.
- Relatively little effort has been devoted to single-crystal  $\text{CuInSe}_2$  devices since the early work, due to, at least in part, the difficulty in growing high-quality crystals.
- The first thin-film  $\text{CuInSe}_2/\text{CdS}$  devices ( $\sim 6 - 7\%$ ) were fabricated in 1976 by Kazmerski *et al.* using films deposited by evaporation of  $\text{CuInSe}_2$  powder along with excess Se.
- Thin-film  $\text{CuInSe}_2$  solar cells began to receive a lot of attention when 9.4%, cells were demonstrated by Mickelsen et al. from Boeing, in 1981.
- With this advance, interest in  $\text{Cu}_2\text{S}/\text{CdS}$  thin-film solar cells waned due to problems related to electrochemical instabilities, and many of these researchers turned their focus to  $\text{CuInSe}_2$ .

After “ $\text{Cu}(\text{InGa})\text{Se}_2$  Solar Cells”, by Shafarman and Stolt, and Wikipedia

From its earliest development, CuInSe<sub>2</sub> was considered promising for solar cells because of its favorable electronic and optical properties including its direct band gap with high absorption coefficient and inherent *p-type conductivity*. As science and technology developed, it also became apparent that it is a very forgiving material since:

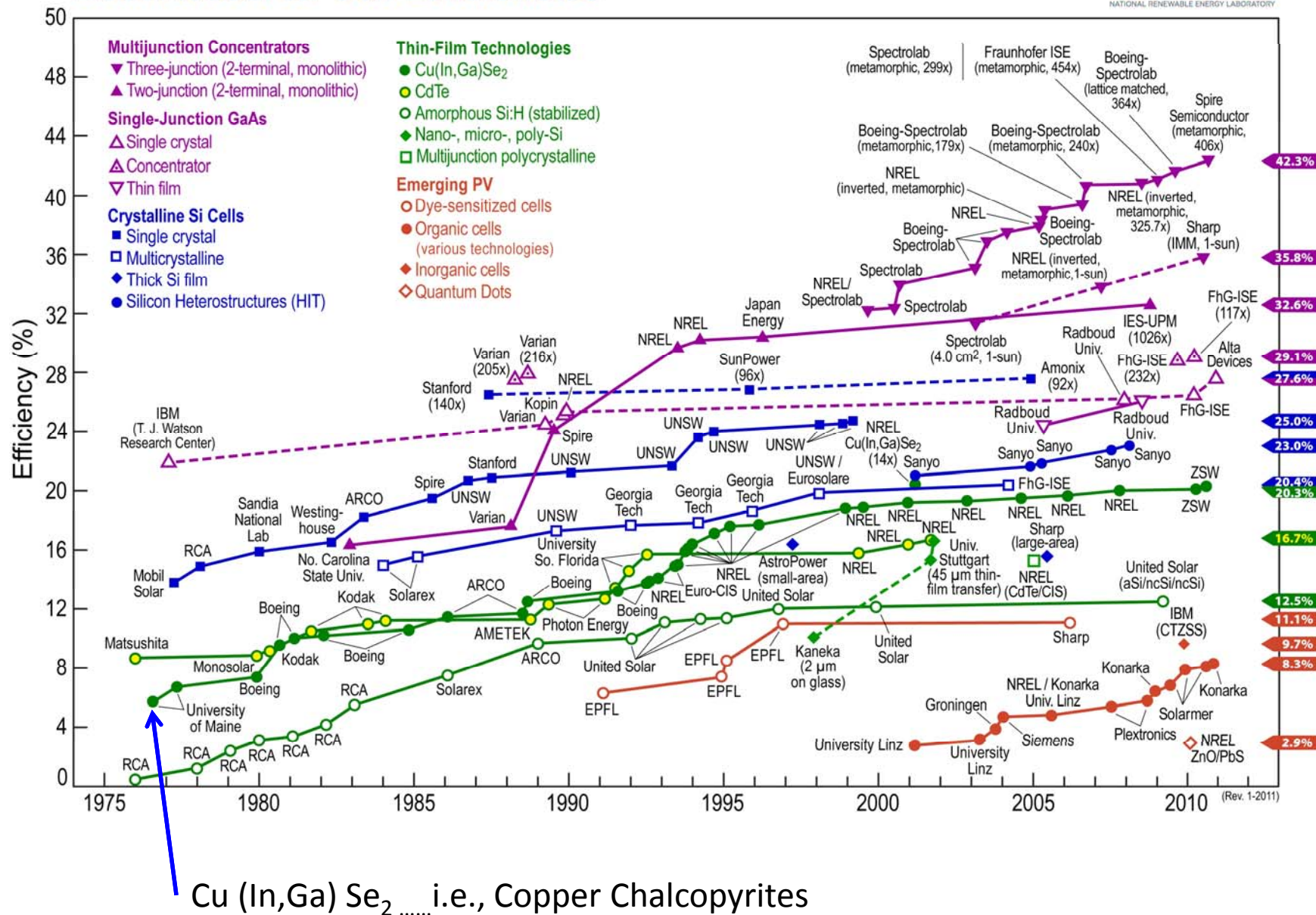
- (1) high efficiency devices can be made with a wide tolerance to variations in Cu(InGa)Se<sub>2</sub> composition,
- (2) grain boundaries are inherently passive so even films with grain sizes less than 1 μm can be used, and
- (3) device behavior is insensitive to defects at the junction caused by a lattice mismatch or impurities between the Cu(InGa)Se<sub>2</sub> and CdS. The latter enables high-efficiency devices to be processed despite exposure of the Cu(InGa)Se<sub>2</sub> to air prior to junction formation.

After “Cu(InGa)Se<sub>2</sub> Solar Cells”, by Shafarman and Stolt, and Wikipedia

- Boeing Devices:
  - CuInSe<sub>2</sub> deposited by co-evaporation, i.e. evaporation from separate elemental sources, onto ceramic substrates coated with a Mo back electrode.
  - Heterojunction partner formed by evaporation of CdS or (CdZn)S in two layers: undoped CdS followed by an In-doped CdS (to aid in current conduction)
- In 1980s, Boeing and ARCO Solar began to address the difficult manufacturing issues related to scale-up, yield, and throughput leading to many advancements in CuInSe<sub>2</sub> solar cell technology.
- These two basic approaches to CuInSe<sub>2</sub> deposition remain the most common deposition methods and produce the highest device and module efficiencies.
- Boeing focused on depositing Cu(InGa)Se<sub>2</sub> by **co-evaporation**,
- ARCO Solar focused on a **two-stage process** of Cu and In deposition at a low temperature followed by a reactive anneal in H<sub>2</sub>Se.

After “Cu(InGa)Se<sub>2</sub> Solar Cells”, by Shafarman and Stolt, and Wikipedia

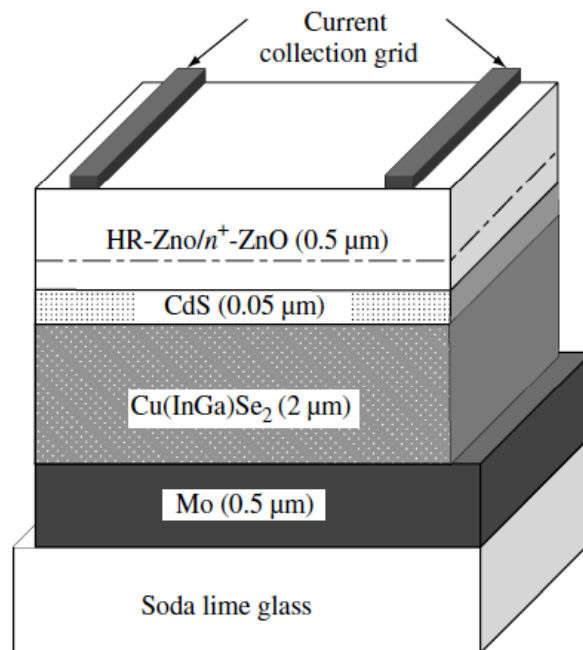
# Best Research-Cell Efficiencies



All the solar cells have the same basic cell structure built around a Cu(InGa)Se<sub>2</sub>/CdS junction in a substrate configuration.

Soda lime glass substrate, coated with a sputtered Mo layer as a back contact.

After the Cu(InGa)Se<sub>2</sub> deposition, the junction is formed by chemical bath–deposited CdS with thickness  $\leq 50$  nm. Then a high-resistance (HR) ZnO and a doped high-conductivity ZnO layer are deposited, usually by sputtering or chemical vapor deposition. Either a current-collecting grid or monolithic series interconnection completes the device or module, respectively.



Schematic cross section of a typical Cu(InGa)Se<sub>2</sub> solar cell

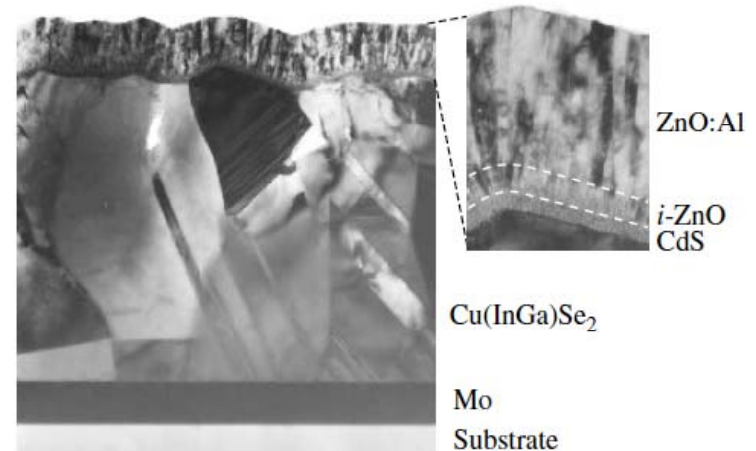
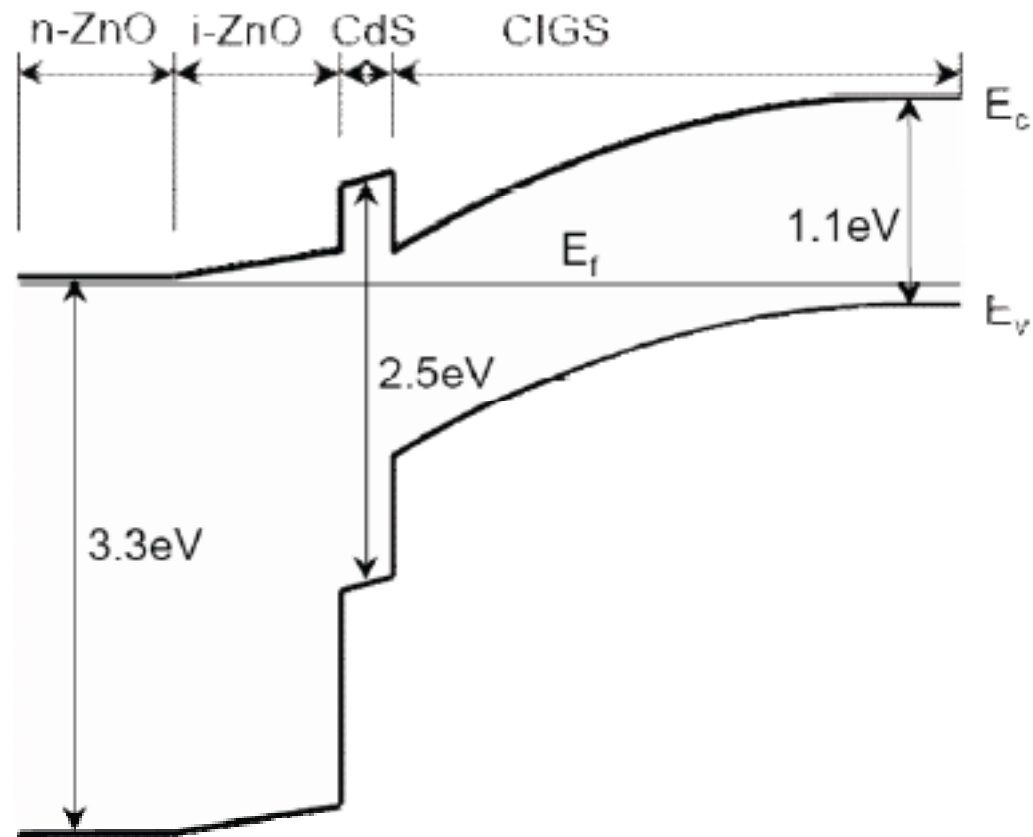


Figure 13.2 TEM cross section of a Cu(InGa)Se<sub>2</sub> solar cell

After “Cu(InGa)Se<sub>2</sub> Solar Cells”, by Shafarman and Stolt, and Wikipedia



[http://www.tf.uni-kiel.de/matwis/amat/matissem\\_en/kap\\_6/illistr/gerngross\\_reverey\\_paper\\_ws\\_08\\_1.pdf](http://www.tf.uni-kiel.de/matwis/amat/matissem_en/kap_6/illistr/gerngross_reverey_paper_ws_08_1.pdf)

The basic solar cell configuration implemented by Boeing provided the basis for a series of improvements that have lead to the high-efficiency device technology of today.

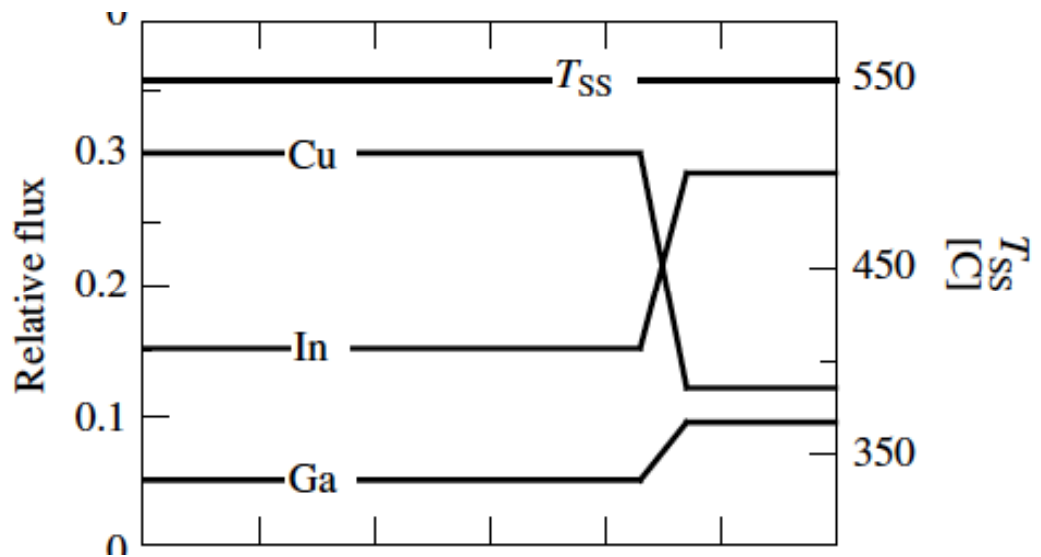
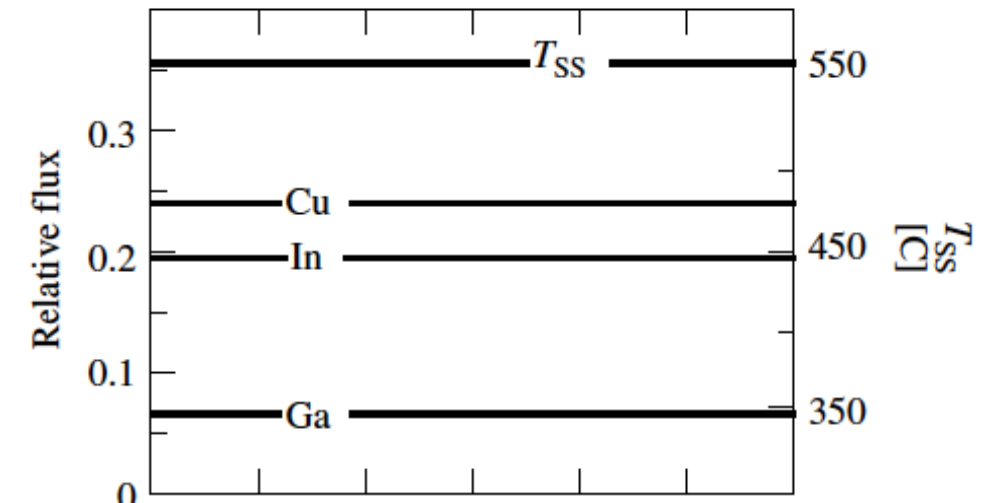
The most important of these improvements to the technology include the following:

- (1) The absorber-layer band gap was increased from 1.02 eV for CuInSe<sub>2</sub> to 1.1–1.2 eV by the partial substitution of In with Ga, leading to a substantial increase in efficiency [Chen et al., 1987].
- (2) The 1- to 2-μm-thick doped (CdZn)S layer was replaced with a thin, ≤50 nm, undoped CdS and a conductive ZnO current-carrying layer [Potter, 1986]. This increased the cell current by increasing the short wavelength (blue) response.
- (3) Soda lime glass replaced ceramic or borosilicate glass substrates. Initially, this change was made for the lower costs of the soda lime glass and its good thermal expansion match to CuInSe<sub>2</sub>. However, it soon became clear that an increase in device performance and processing tolerance resulted primarily from the beneficial indiffusion of sodium from the glass [Hedstrom, 1993].
- (4) Advanced absorber fabrication processes were developed that incorporate band gap gradients that improve the operating voltage and current collection [Gabor, 1996, Tarrant, 1993].

After “Cu(InGa)Se<sub>2</sub> Solar Cells”, by Shafarman and Stolt, and Wikipedia

Simplest stationary process: all fluxes are constant.

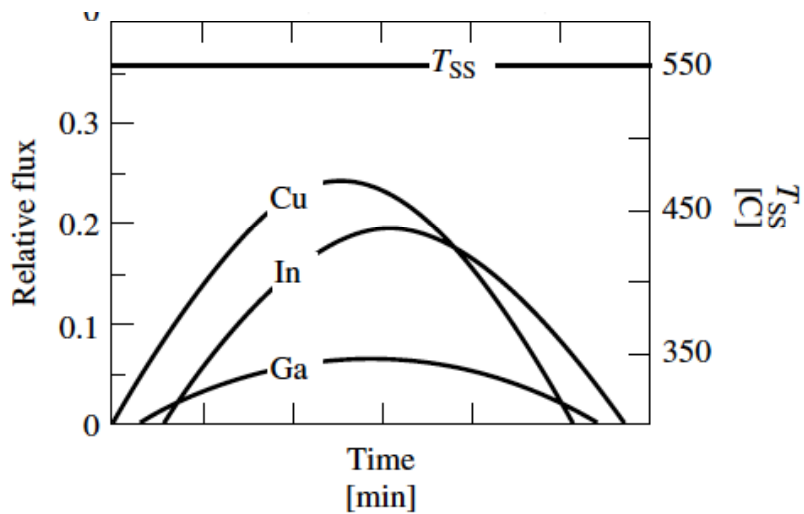
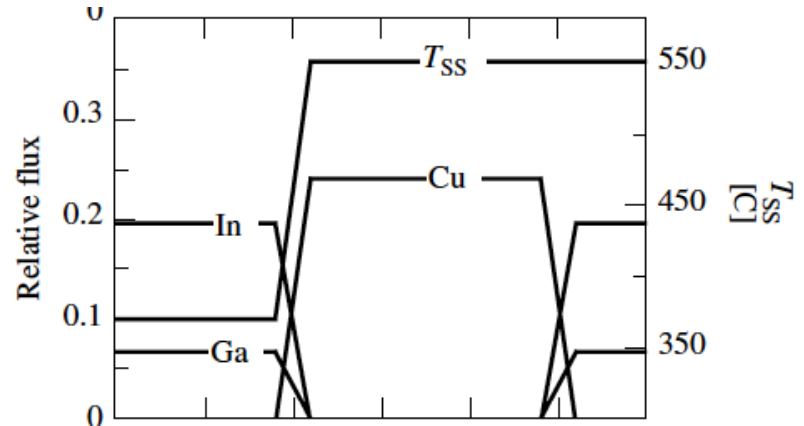
“the Boeing process” - the bulk of the film is grown to be Cu rich in overall composition so that it contains a *CuxSe phase in addition to Cu(InGa)Se<sub>2</sub>*. The fluxes are then adjusted to finish the deposition with In- and Ga-rich flux so that the final film composition has the desired Cu-deficient composition.



After “Cu(InGa)Se<sub>2</sub> Solar Cells”, by Shafarman and Stolt, and Wikipedia

In and Ga are deposited separately initially to form a an  $(\text{InGa})_x\text{Se}_y$  compound, followed by the deposition of Cu and Se until the growing film reaches the desired composition. The layers interdiffuse to form the  $\text{Cu}(\text{InGa})\text{Se}_2$  film. Gabor *et al.* allowed the Cu flux to reach an overall Cu-rich composition. Then a third step is added to the process in which In and Ga, again in the presence of excess Se, are evaporated to bring the composition back to Cu-deficient. The metals interdiffuse, forming the ternary chalcopyrite film. This process produces the highest efficiency, due band gap grading and improved crystallinity.

### Process on moving belt

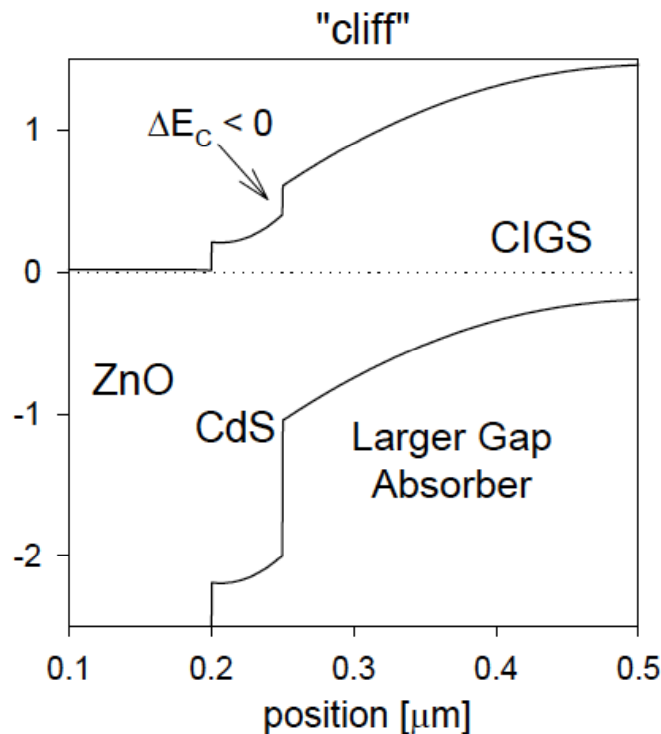
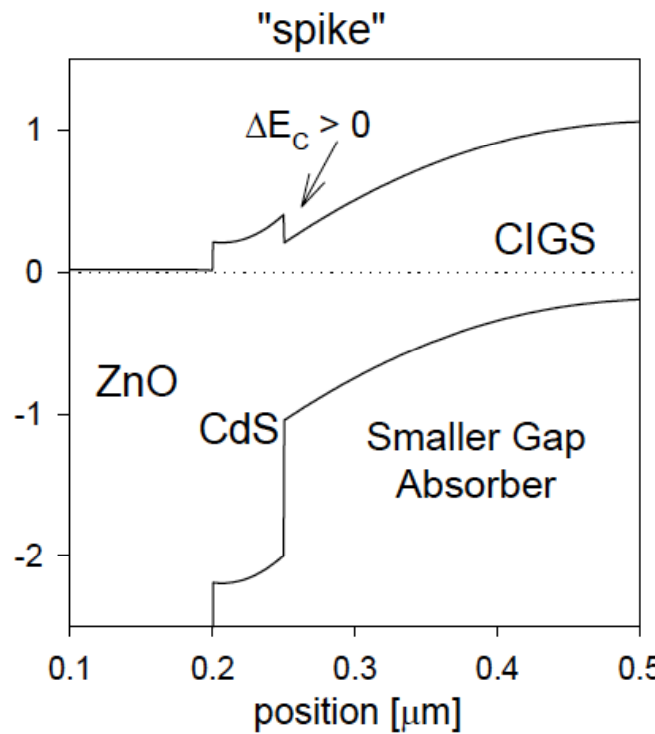


After “ $\text{Cu}(\text{InGa})\text{Se}_2$  Solar Cells”, by Shafarman and Stolt, and Wikipedia

# Sign Convention for $\Delta E_c$

---

---



Spike can impede photoelectrons (may be bad)

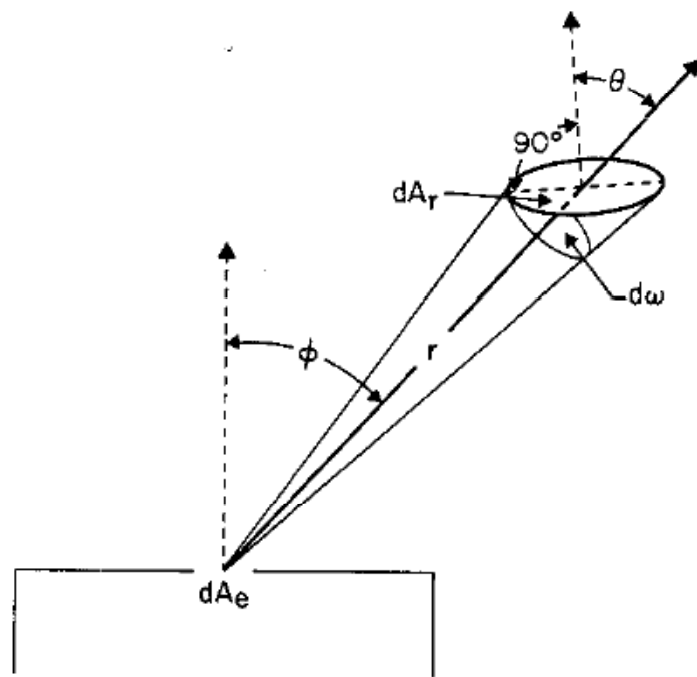
Cliff slows forward electrons in interfacial-recombination region (also may be bad)

Some consensus on  $\Delta E_c$  magnitudes between theory,  
experiment, and numerical simulations of J-V curves

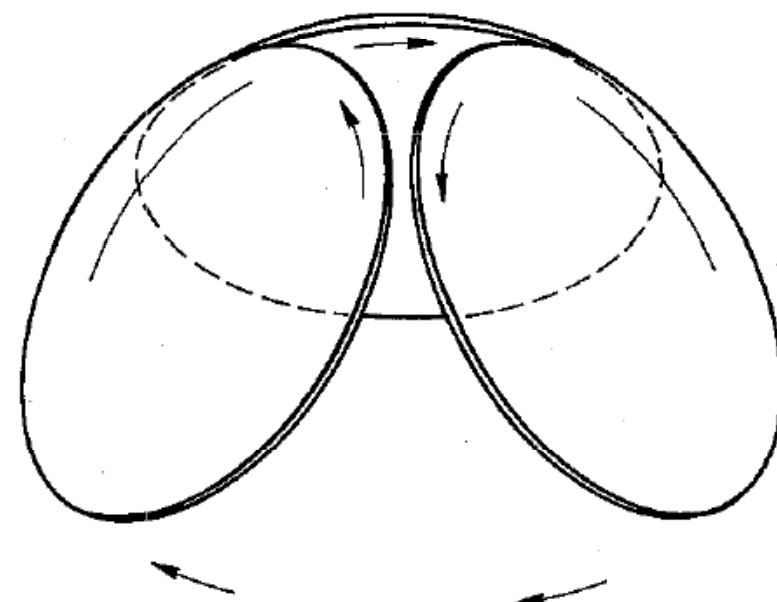
- EC's in-line evaporation system for the deposition of Cu(InGa)Se<sub>2</sub> on a moving substrate can be used with flexible web (plastic or metal foil) in a roll-to-roll configuration or with glass substrates.



## *Evaporation Control*

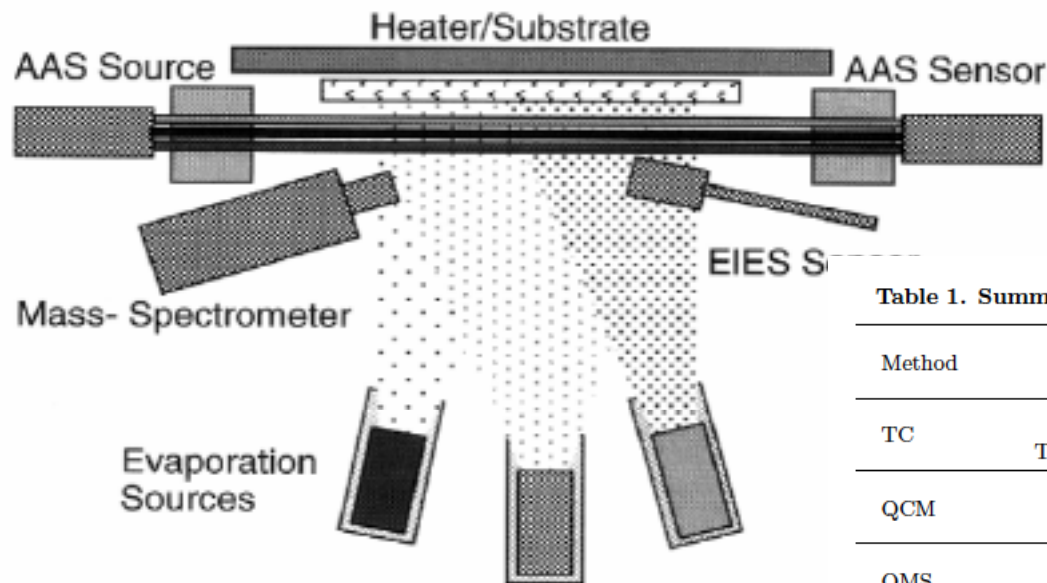


**Evaporation Geometry**



**Substrate Motion**

Sze, Figs. 4, 5, p. 394-95



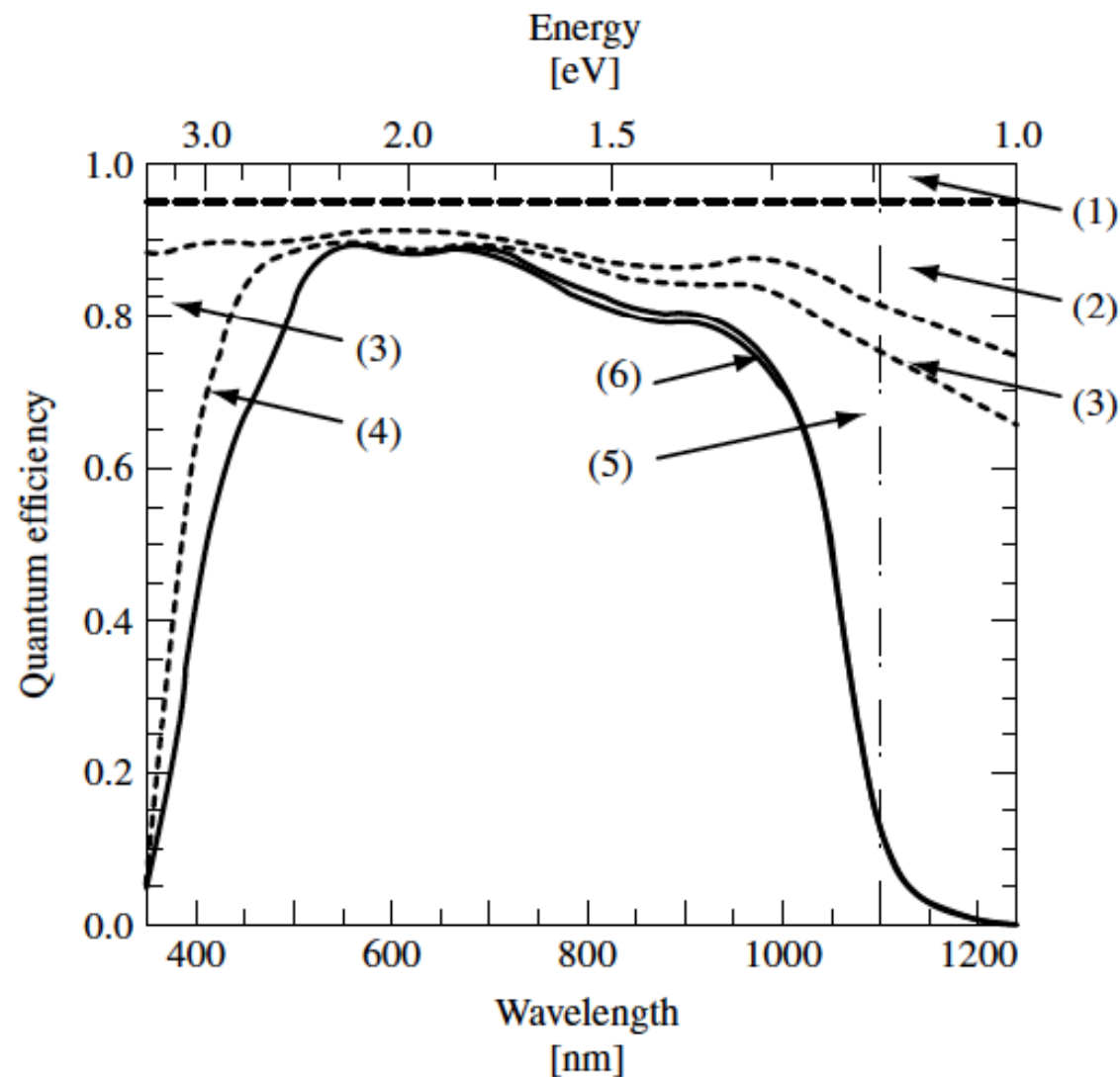
[http://www.tf.uni-kiel.de/matlwis/amat/matlwissem\\_en/kap\\_6/illistr/gerngross\\_reverey\\_paper\\_ws\\_08\\_1.pdf](http://www.tf.uni-kiel.de/matlwis/amat/matlwissem_en/kap_6/illistr/gerngross_reverey_paper_ws_08_1.pdf)

Table 1. Summary of Process Monitors Currently Used in CIGS Co-Evaporation

Method	Probe	Features	System	Cost	Commercially Available
TC	Source Temperature	Rate of One Element	Lab, Industry	\$	Yes
QCM	Quartz Crystal	Rate of One Element	Lab	\$\$	Yes
QMS	Mass Ion	Flux of Multiple Elements	Lab	\$\$\$	Yes
TC	Heat Radiation	Composition	Lab	\$	Yes
TC Pyrometer	Heat Radiation	Composition, Thickness	Lab	\$\$	Yes
Infrared Monitor	Heat Radiation	Composition, Thickness	Lab	\$\$	Yes
SLS	White Light	Composition, Thickness, Surface Structure, Band gap	Lab	\$\$\$	No
SE	Polarized Light	Composition, Thickness, Surface Structure, Band gap	Lab, Industry	\$\$\$	No
EIES	Atomic Emission	Flux of Multiple Elements	Lab	\$\$\$	Yes
AA	Atomic Absorption	Flux of Multiple Elements	Lab, Industry	\$\$\$	Yes
XRF	X-ray	Composition, Thickness	Lab, Industry	\$\$\$	Yes

From CHINESE OPTICS LETTERS / Vol. 8, Supplement / April 30, 2010  
*In situ optical monitor system for CIGS solar cell applications, Fan and Nagai*

# Losses in the spectral response of the device (current losses)



After “Cu(InGa)Se<sub>2</sub> Solar Cells”, by Shafarman and Stolt, and Wikipedia

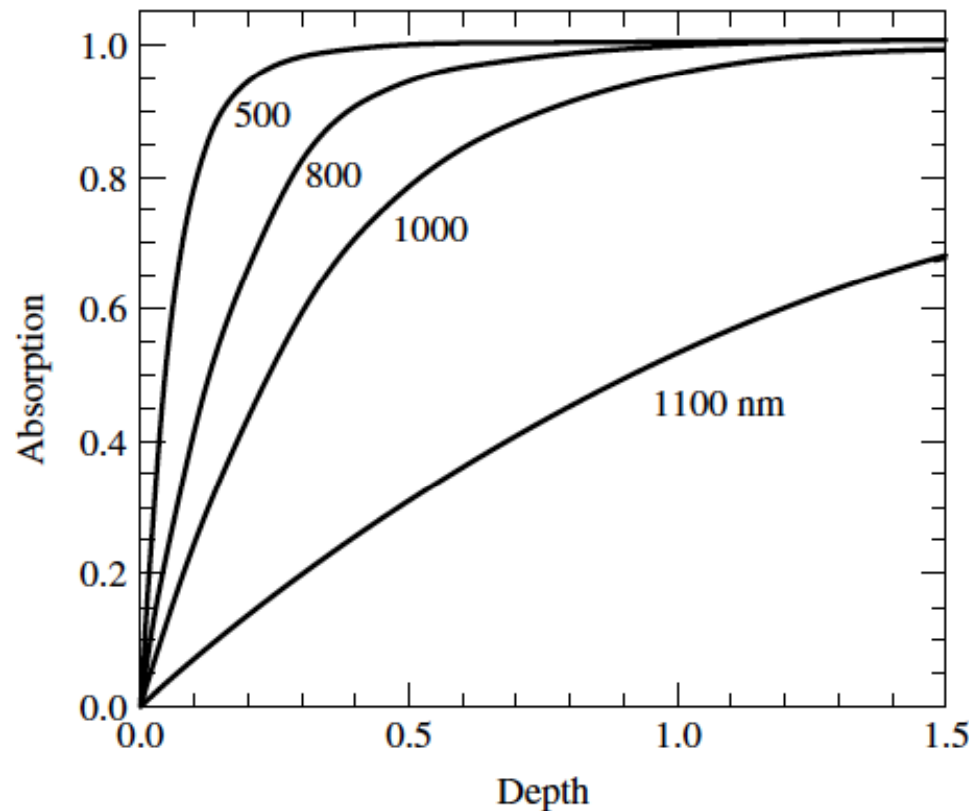
# Current losses

1. Shading from a collection grid used for most devices. In an interconnected module this will be replaced by the area used for the interconnect, as discussed in Section 13.6.2.
2. Front surface reflection. On the highest-efficiency devices this is minimized with an antireflection layer for which an evaporated MgF<sub>2</sub> layer with thickness  $\sim 100$  nm is commonly used. However, this is not practical in a module in which a cover glass is typically required.
3. Absorption in the TCO layer. Typically, there is 1 to 3% absorption through the visible wavelengths, which increases in the near IR region,  $\lambda > 900$  nm, where free-carrier absorption becomes significant, and for  $\lambda < 400$  nm near the ZnO band gap.
4. Absorption in the CdS layer. This becomes appreciable at wavelengths below  $\sim 520$  nm corresponding to the CdS band gap 2.42 eV. The loss in QE for  $\lambda < 500$  nm is proportional to the CdS thickness since it is commonly assumed that electron–hole pairs generated in the CdS are not collected. Figure 13.14 shows a device with a  $\sim 30$  nm-thick CdS layer. In practice, the CdS layer is often thicker and the absorption loss greater.
5. Incomplete absorption in the Cu(InGa)Se<sub>2</sub> layer near the Cu(InGa)Se<sub>2</sub> band gap. Band gap gradients, resulting from composition gradients in many Cu(InGa)Se<sub>2</sub> films, also affect the steepness of the long-wavelength part of the QE curve. If the Cu(InGa)Se<sub>2</sub> is made thinner than  $\sim 1.0$   $\mu\text{m}$ , this loss becomes significant [163] because of insufficient absorption at long wavelengths.

$$QE_{\text{ext}}(\lambda, V) = [1 - R(\lambda)][1 - A_{\text{ZnO}}(\lambda)][1 - A_{\text{CdS}}(\lambda)] QE_{\text{int}}(\lambda, V)$$

After “Cu(InGa)Se<sub>2</sub> Solar Cells”, by Shafarman and Stolt, and Wikipedia

# Depletion width losses in thin cells



Absorption of light with different wavelengths in  $\text{Cu}(\text{InGa})\text{Se}_2$  with  $x = 0.2$

After “ $\text{Cu}(\text{InGa})\text{Se}_2$  Solar Cells”, by Shafarman and Stolt, and Wikipedia

# Current losses

**Table 13.4** Current loss,  $\Delta J$ , for  $E > 1.12$  eV due to the optical and collection losses illustrated in Figure 13.14 for a typical Cu(InGa)Se<sub>2</sub>/CdS solar cell

Region in Figure 13.14	Optical loss mechanism	$\Delta J$ [mA/cm <sup>2</sup> ]
(1)	Shading from grid with 4% area coverage	1.7
(2)	Reflection from Cu(InGa)Se <sub>2</sub> /CdS/ZnO	3.8
(3)	Absorption in ZnO	1.8
(4)	Absorption in CdS	0.8
(5)	Incomplete generation in Cu(InGa)Se <sub>2</sub>	1.9
(6)	Incomplete collection in Cu(InGa)Se <sub>2</sub>	0.4

After “Cu(InGa)Se<sub>2</sub> Solar Cells”, by Shafarman and Stolt, and Wikipedia

## CIGS – other deposition approaches

- Co-evaporation and the 2-step process have been identified as potential low-cost alternatives for manufacturing, and have been dominant in recent research.
- Other techniques that have been explored:
  - Reactive sputtering
  - Hybrid sputtering in which Cu, In, and Ga are sputtered while Se is evaporated
  - Closed space sublimation (CSS)
  - Chemical bath deposition (CBD)
  - Laser evaporation
  - Spray pyrolysis (heat treatment / annealing in the presence of a reducing gas such as hydrogen).

**Cu(InGa)Se<sub>2</sub> Solar Cells, by William N. Shafarman<sup>1</sup> and Lars Stolt<sup>2</sup>**

<sup>1</sup>*University of Delaware, Newark, DE, USA*, <sup>2</sup>*Uppsala University, Uppsala, Sweden*

*Handbook of Photovoltaic Science and Engineering. Edited by A. Luque and S. Hegedus*

2003 John Wiley & Sons, Ltd ISBN: 0-471-49196-9

## Roll-to-roll processing from solution source (e.g., Nanosolar)

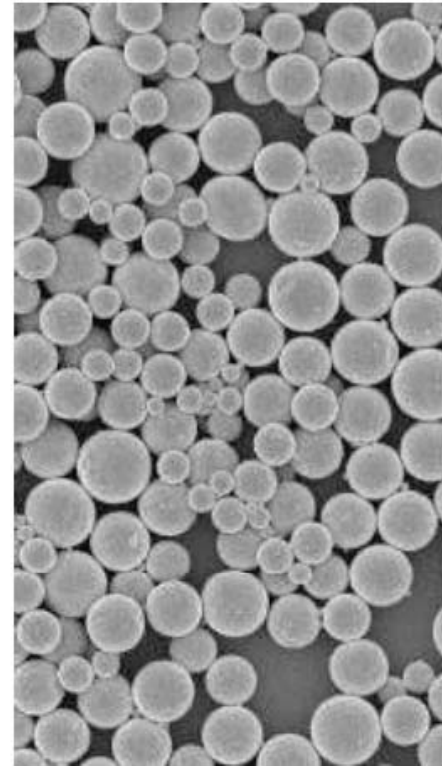


**Figure 6 and 7:** A laboratory sample of our nanoparticle ink. Nanoparticles shown to the right are an average of 20nm in diameter.

from NanoSolar white paper

## Roll-to-roll processing from solution source (e.g., Nanosolar)

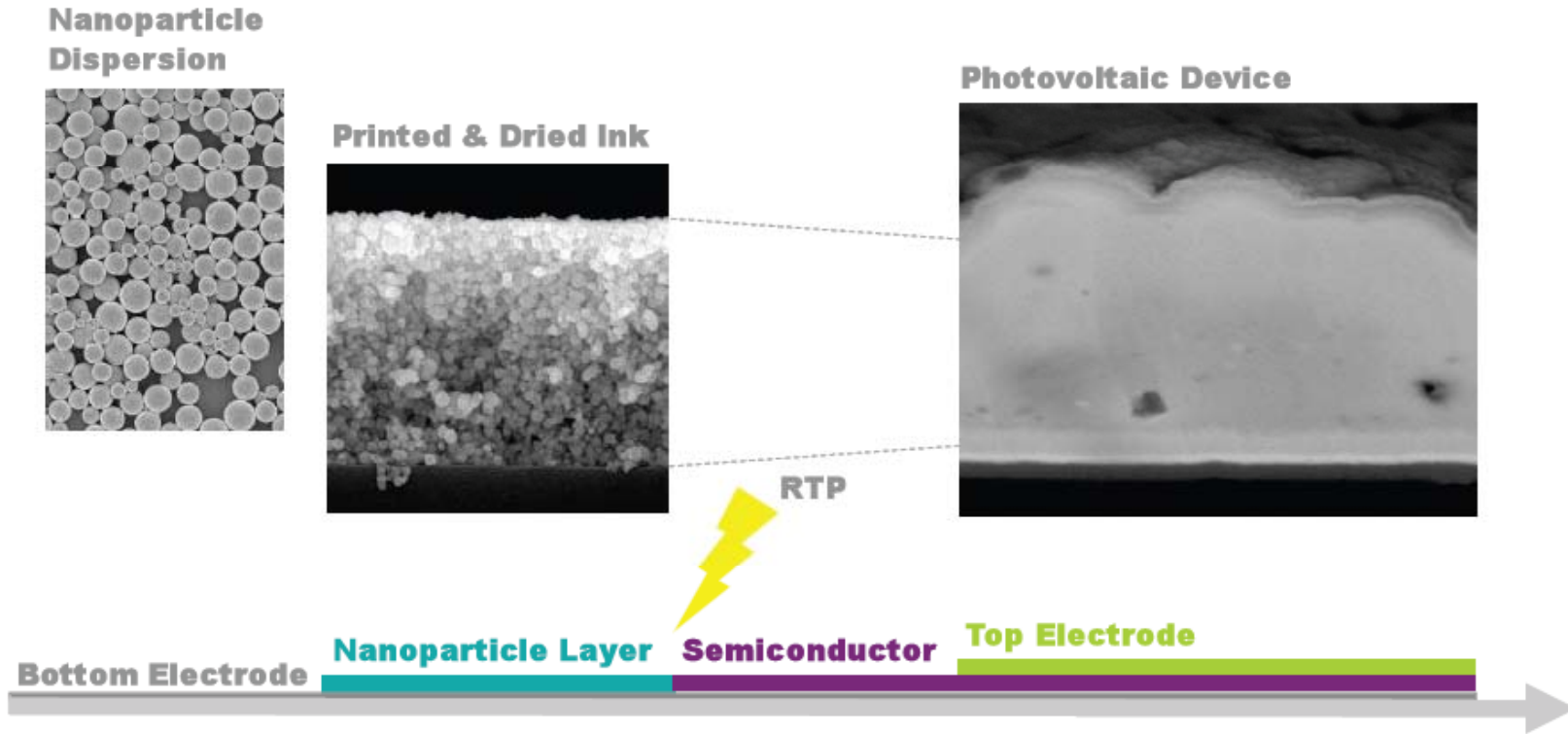


**Figure 8:** The basic process sequence consists of creating a high-quality dispersion of nanoparticles suitable for high-quality wet coating and converting the printed layer into a high-quality semiconductor using Rapid Thermal Processing (RTP). The art consists of doing so in a way that the resulting semiconductor is indistinguishable in electronic and crystalline quality from one deposited with far more expensive high-vacuum deposition techniques.

from NanoSolar white paper

## Roll-to-roll processing from solution source (e.g., Nanosolar)

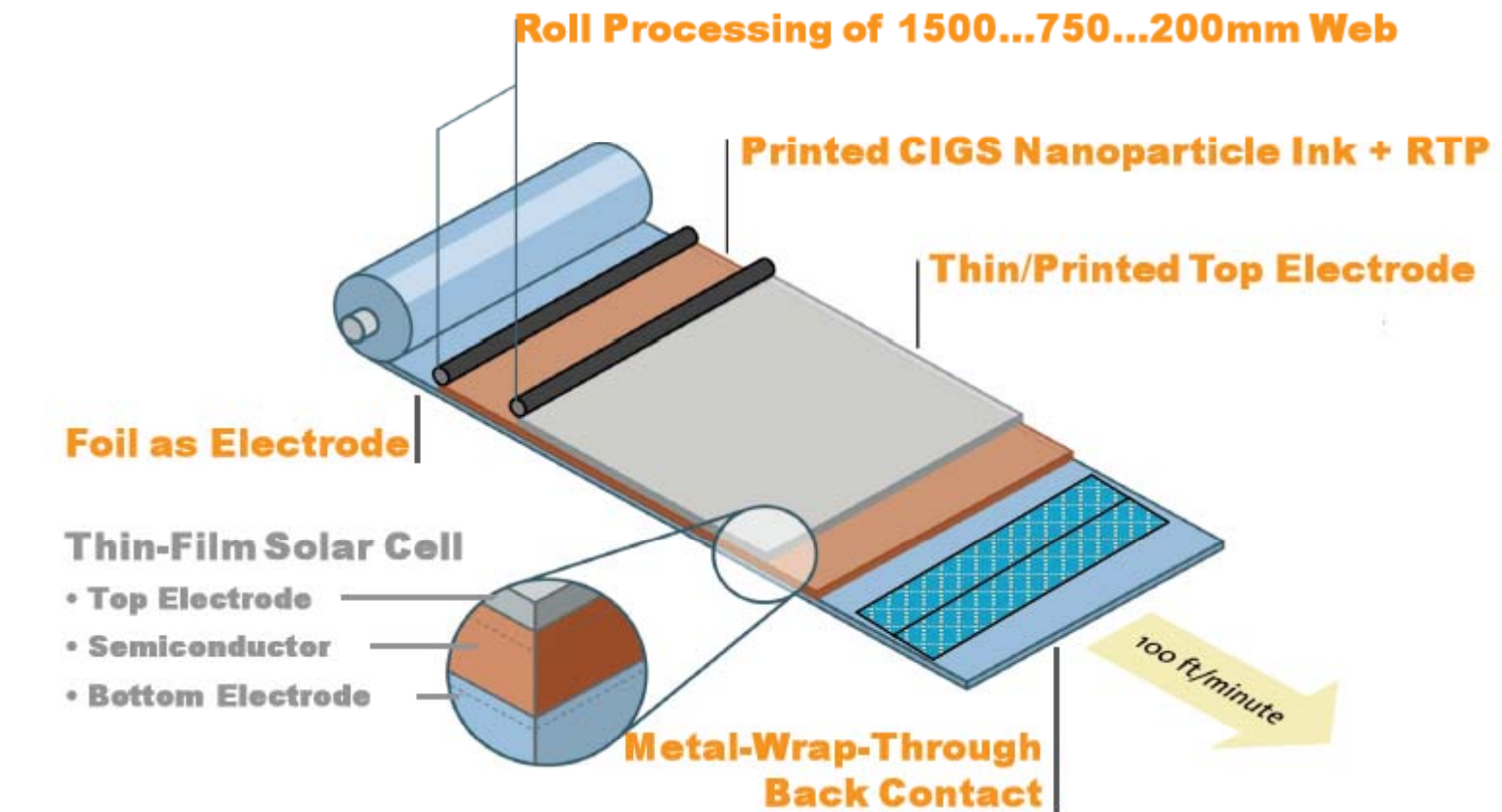


**Figure 1:** Nanosolar combines a host of innovations to deliver a distinct overall cost reduction.

from NanoSolar white paper

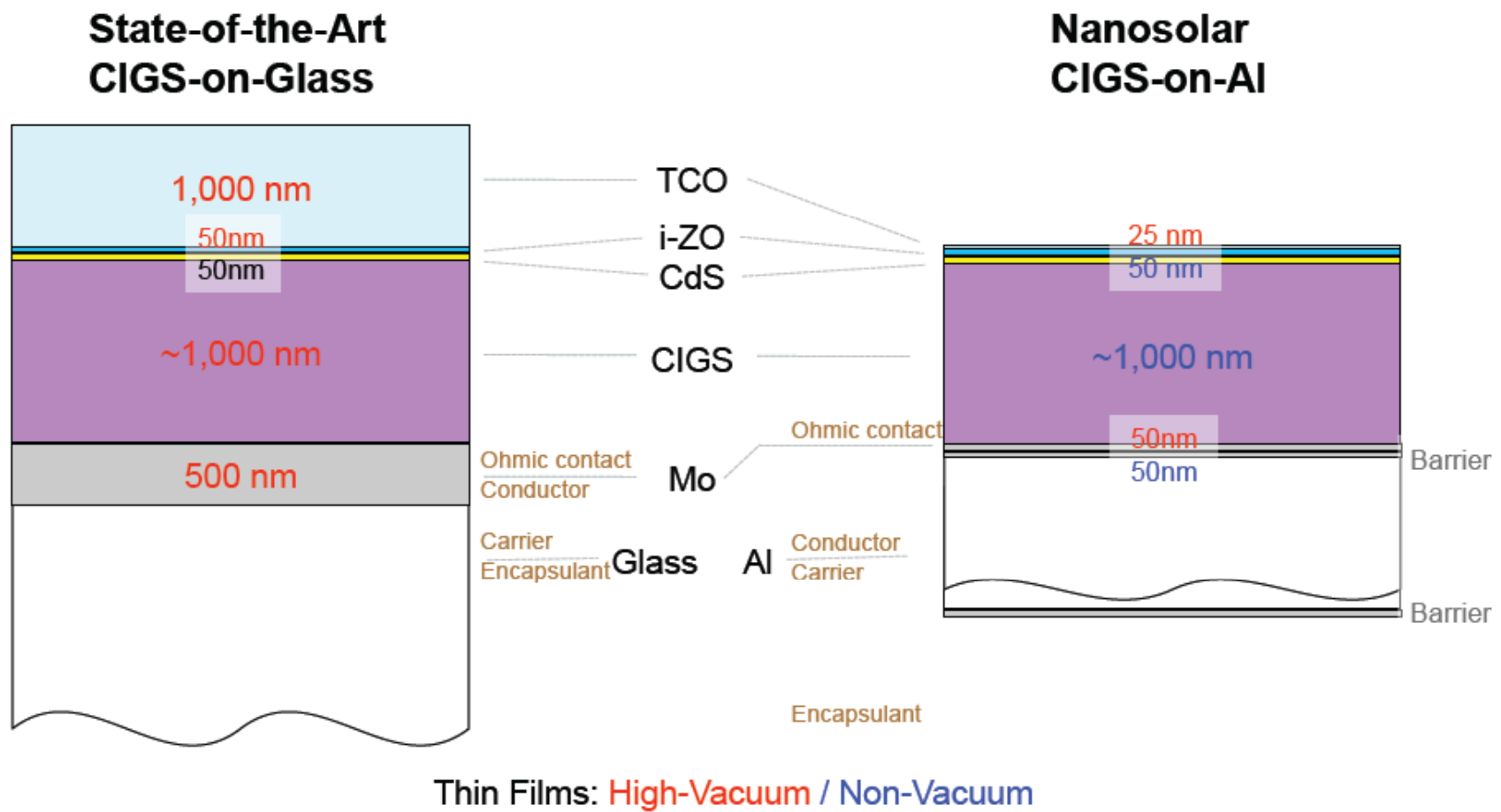


**Figure 4:** Comparison of State-of-the-Art CIGS versus Nanosolar's CIGS-on-Aluminum. Thickness numbers in red indicate depositions using a high-vacuum deposition technique. The state-of-the-art stack requires close to 3000nm of high-vacuum processing whereas Nanosolar's stack requires less than a tenth of that.

from NanoSolar white paper



**Figure 9:** A Nanosolar roll-to-roll processing tool for rapid semiconductor formation, San Jose, California.

from NanoSolar white paper

# Nanosolar

## CdS/Cu(In,Ga)Se<sub>2</sub> Cell

Device ID: H09B071-01C #2

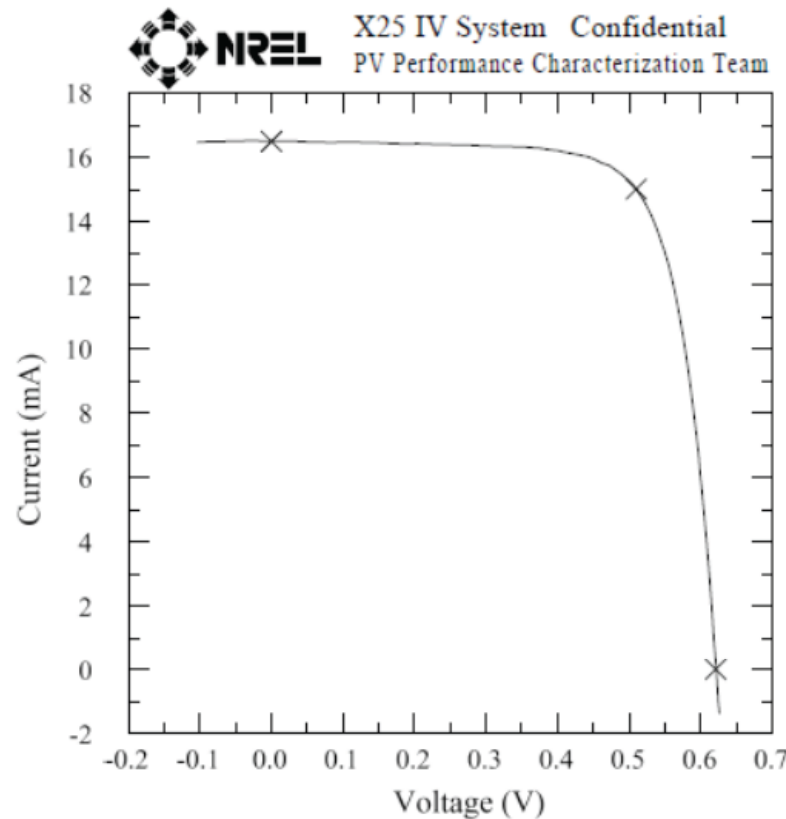
Apr 09, 2009 12:31

Spectrum: ASTM G173 global

Device Temperature: 24.0

Device Area: 0.5000 cm<sup>2</sup>

Irradiance: 1000.0 W/m<sup>2</sup>



$V_{oc} = 0.6214$  V  
 $I_{sc} = 16.490$  mA  
 $J_{sc} = 32.980$  mA/cm<sup>2</sup>  
Fill Factor = 74.70 %

$I_{max} = 15.010$  mA  
 $V_{max} = 0.5101$  V  
 $P_{max} = 7.6540$  mW  
Efficiency = 15.31 %

from NanoSolar white paper

## Substrate considerations for CIGS (key issues)

- Earlier CIS or CIGS devices were fabricated on borosilicate glass. Switching to less-expensive soda lime glass, the solar cells worked better (i.e., higher efficiency).
- *Why does soda lime glass work well for CIS / CIGS?*
- **Coefficient of thermal expansion:** deposition done at a substrate temperature  $T_{ss} > 350 \text{ }^{\circ}\text{C}$  and as high as  $T_{ss} \sim 550 \text{ }^{\circ}\text{C}$  (close to the glass transition temp of  $\sim 564 \text{ }^{\circ}\text{C}$ ). Subsequent cooling of the substrate introduces significant strain if coefficient of thermal expansion differ for the thin film and the substrate. Fortunately, soda lime glass has a value for the thermal expansion coefficient of 9.5 (ppm/K); the value for CIS is  $\sim 8$  ppm/K. In contrast, borosilicate glass has a value of 4.6 ppm/K.
- Soda lime glass includes oxides such as  $\text{Na}_2\text{O}$ ,  $\text{K}_2\text{O}$ , and  $\text{CaO}$ , which provide **sources of alkali impurities** which diffuse into the Mo and  $\text{Cu}(\text{InGa})\text{Se}_2$  films resulting in beneficial defect effects.
- Alkalai impurities are better introduced through a controlled source, so now the glass is coated with a Na diffusion barrier such as  $\text{SiO}_x$  or  $\text{Al}_2\text{O}_3$ .
- “The chalcopyrite phase field is increased by the addition of Ga or Na.” This means that the desirable phase of CIS (or CIGS) is more easily achieved in the presence of Na.

**$\text{Cu}(\text{InGa})\text{Se}_2$  Solar Cells, by William N. Shafarman<sup>1</sup> and Lars Stolt<sup>2</sup>**

<sup>1</sup>*University of Delaware, Newark, DE, USA*, <sup>2</sup>*Uppsala University, Uppsala, Sweden*

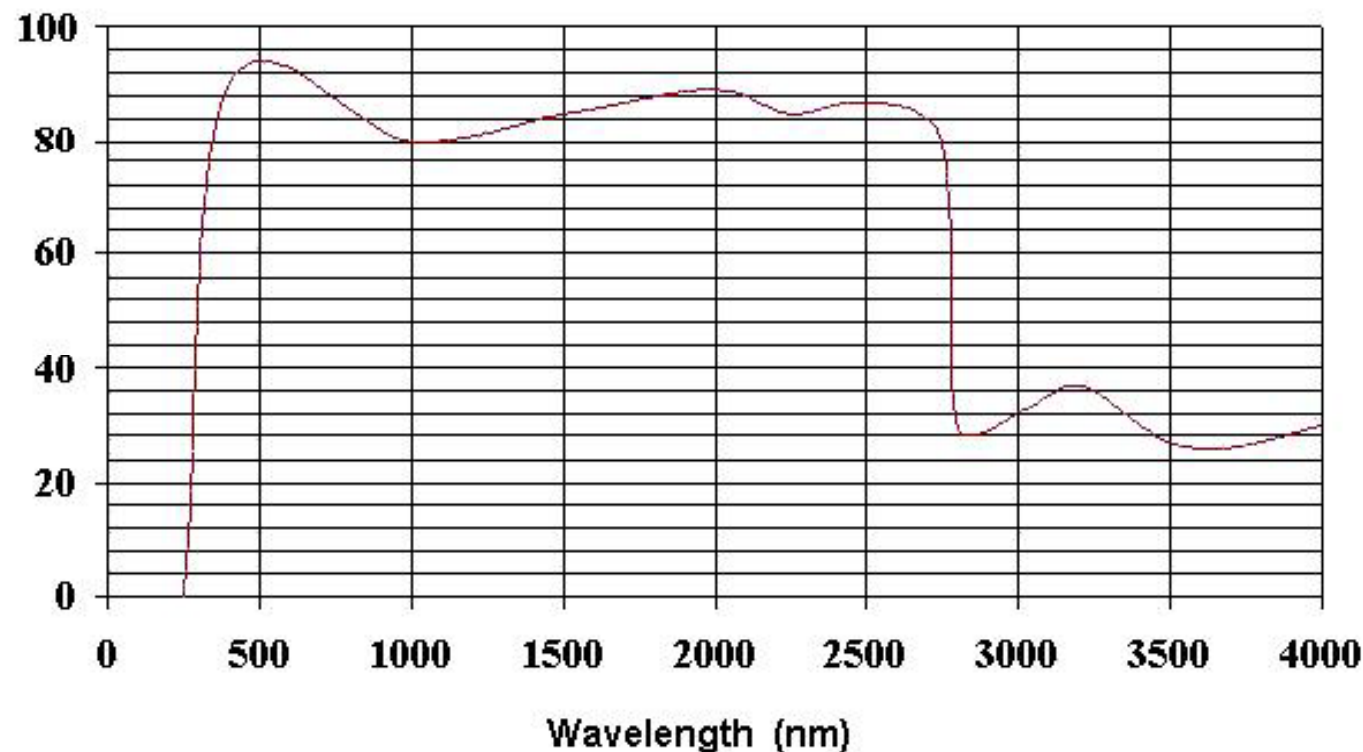
*Handbook of Photovoltaic Science and Engineering. Edited by A. Luque and S. Hegedus*

2003 John Wiley & Sons, Ltd ISBN: 0-471-49196-9

## Soda lime glass transmission

### Soda lime Glass

Transmission %



[http://en.wikipedia.org/wiki/File:Soda\\_Lime.jpg](http://en.wikipedia.org/wiki/File:Soda_Lime.jpg)

## Soda lime glass properties

Properties	Soda-lime glass for windows
Chemical composition, (wt%)	73 SiO <sub>2</sub> , 14 Na <sub>2</sub> O, 9 CaO, 4 MgO, 0.15 Al <sub>2</sub> O <sub>3</sub> , 0.03 K <sub>2</sub> O, 0.02 TiO <sub>2</sub> , 0.1 Fe <sub>2</sub> O <sub>3</sub>
Glass transition temperature, T <sub>g</sub> , °C	564
Coefficient of thermal expansion, ppm/K, ~100-300°C	9.5
Refractive index, n <sub>D</sub> at 20°C	1.520
Heat capacity at 20°C, J/(mol·K)	48

## CIGS back contact (molybdenum, Mo)

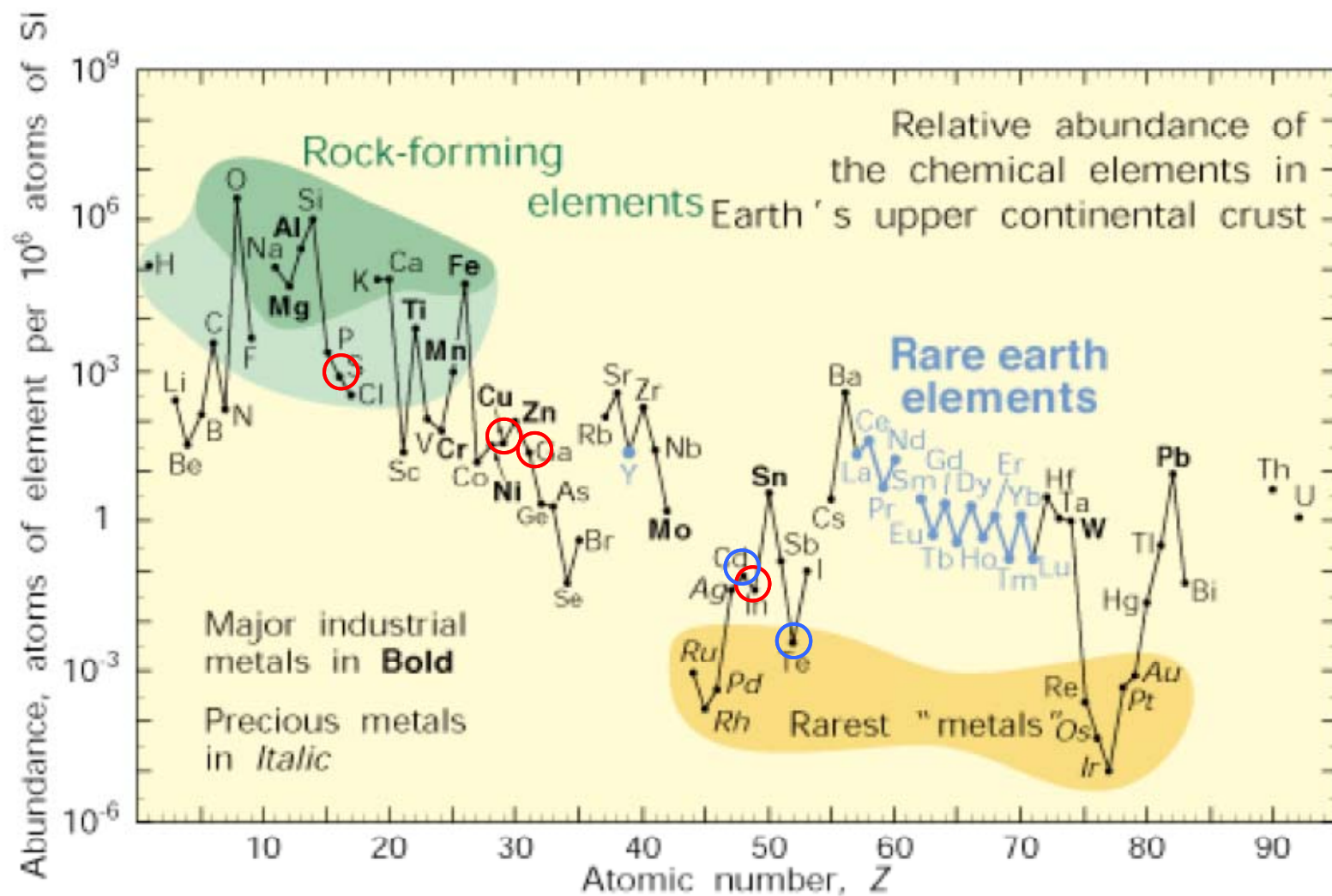
- All high-efficiency CIS and CIGS devices use Mo as the back contact.
- Typically deposited DC sputtering.
- Cell or module configuration determines required thickness (1  $\mu\text{m}$  gives a sheet resistance of 0.1 to 0.2  $\Omega / \square$ , *a factor of 2 to 4 higher resistivity than bulk Mo*).
- Sputter deposition requires careful control of the pressure to control stress in the film, to avoid adhesion.
- During Cu(InGa)Se<sub>2</sub> deposition, a MoSe<sub>2</sub> layer forms at the interface, with properties influenced by the Mo film (less MoSe<sub>2</sub> forms on dense Mo). Metals other than Mo have been investigated with limited success.

**Cu(InGa)Se<sub>2</sub> Solar Cells, by William N. Shafarman<sup>1</sup> and Lars Stolt<sup>2</sup>**

<sup>1</sup>*University of Delaware, Newark, DE, USA*, <sup>2</sup>*Uppsala University, Uppsala, Sweden*

*Handbook of Photovoltaic Science and Engineering. Edited by A. Luque and S. Hegedus*

2003 John Wiley & Sons, Ltd ISBN: 0-471-49196-9



Abundance (atom fraction) of the chemical elements in Earth's upper continental crust as a function of atomic number. Many of the elements are classified into (partially overlapping) categories: (1) rock-forming elements (major elements in green field and minor elements in light green field); (2) rare earth elements (lanthanides, La–Lu, and Y; labeled in blue); (3) major industrial metals (global production  $>\sim 3 \times 10^7$  kg/year; labeled in bold); (4) precious metals (italic); and (5) the nine rarest "metals"—the six platinum group elements plus Au, Re, and Te (a metalloid)

Gordon B. Haxel, James B. Hedrick, and Greta J. Orris, Rare Earth Elements—Critical Resources for High Technology, U.S. Geological Survey Fact Sheet 087-02

# State of Commercialization, as of 2003

Several companies worldwide are pursuing the commercial development of Cu(InGa)Se<sub>2</sub>-based modules. The most advanced, having demonstrated excellent reproducibility in its module manufacturing using the two-stage selenization process for Cu(InGa)(SeS)<sub>2</sub> deposition is Shell Solar Industries (SSI) in California, which was formerly ARCO Solar and then Siemens Solar. They are now in production with 5-, 10-, 20-, and 40-W modules that are commercially available.

In Germany, Wurth Solar is in pilot production using an in-line coevaporation process for Cu(InGa)Se<sub>2</sub> deposition and has also reported large area modules with >12% efficiency. In the USA, several companies are in preproduction or pilot production: Energy Photovoltaics, Inc. (EPV) is using its own in-line evaporation process, International Solar Electric Technology (ISET) is developing a particle-based precursor for selenization, and Global Solar Energy (GSE) is pursuing a process for roll-to-roll coevaporation onto a flexible substrate. In Japan, Showa Shell, using a two-stage selenization process, and Matsushita, using coevaporation for Cu(InGa)Se<sub>2</sub> deposition, are also in production development stages.

Despite the level of effort on developing manufacturing processes, there remains a large discrepancy in efficiency between the laboratory-scale solar cells and minimodules, and the best full-scale modules. In part, this is due to the necessity for developing completely new processes and equipment for the large-area, high-throughput deposition needed for manufacturing thin-film photovoltaics. This is compounded by the lack of a comprehensive scientific base for Cu(InGa)Se<sub>2</sub> materials and devices, due partly to the fact that it has not attracted a broader interest for other applications. This lack of a science base has been perhaps the biggest hindrance to the maturation of Cu(InGa)Se<sub>2</sub> solar cell technology as most of the progress has been empirical. Still, in many areas a deeper understanding has emerged in the recent years.

After “Cu(InGa)Se<sub>2</sub> Solar Cells”, by Shafarman and Stolt, and Wikipedia